

# Characterization of dislocation loops and chromium-rich precipitates in ferritic iron–chromium alloys as means of void swelling suppression

D. Terentyev<sup>b,\*</sup>, P. Olsson<sup>c</sup>, L. Malerba<sup>a</sup>, A.V. Barashev<sup>d</sup>

<sup>a</sup> SCK-CEN, RMO Department, Boeretang 200, B-2400, Mol, Belgium

<sup>b</sup> Physique des Solides Irradiés et des Nanostructures CP23, Université Libre de Bruxelles, Bd du Triomphe B-1050, Brussels, Belgium

<sup>c</sup> Department Matériaux et Mécanique des Composants, Electricité de France, Les Renardières, F-77250 Moret-sur-Loing, France

<sup>d</sup> Department of Engineering, The University of Liverpool, Brownlow Hill, Liverpool, L69 3GH, UK

## Abstract

We have used both *ab initio* and empirical potential based molecular dynamics and static calculations to parameterize a model accounting for the mobility of self-interstitial clusters and small dislocation loops in Fe–Cr alloys depending on Cr content. Particularly, we have considered the interval of 5–15% of Cr, corresponding to the typical concentration of Cr in ferritic/martensitic steels. The mobility of self-interstitial clusters and small dislocation loops was found to be strongly reduced in the presence of Cr due to attractive interaction between self-interstitials and Cr atoms, whereas Cr-rich precipitates act as repulsive obstacles. The results obtained allow the experimental trend of swelling measurements in neutron and high-energy electron irradiated Fe–Cr alloys to be interpreted and explained.

© 2007 Elsevier B.V. All rights reserved.

PACS: 75.50.Bb; 61.82.Bg; 81.30.Mh; 66.30.Lw

## 1. Introduction

Void swelling in metals and alloys under irradiation has been studied for the last 40 years [1]. The basic mechanisms of void formation can be rationalized in the framework of the production bias model in pure metals, which ascribes swelling to the removal of atoms from the bulk via fast, one-dimensional (1D) migration of self-interstitial atom

(SIA) clusters produced by irradiation [2]. In the case of Fe–Cr alloys, it is known that the addition of Cr to pure Fe suppresses radiation-induced swelling, typically by an order of magnitude [3–5]. Specifically, swelling drastically decreases with the addition of small quantities of Cr, remains low for concentrations ( $C_{Cr}$ ) between 1% and 10% and then rises again. At higher irradiation doses, the swelling curve evolves and exhibits a local maximum at ~9% Cr and then two local minima at about 3% and 15% Cr. Above this Cr content swelling may or may not increase, depending on irradiation conditions [5]. This peculiar swelling behaviour has not been fully

\* Corresponding author. Tel.: +32 14 333197; fax: +32 14 321216.

E-mail address: [dterenty@sckcen.be](mailto:dterenty@sckcen.be) (D. Terentyev).

explained yet. A possible reason for low swelling in ferritic alloys has been identified in the presence of two types of dislocation loops, namely  $1/2 a\langle 111 \rangle$  and  $a\langle 100 \rangle$ , characterized by different bias towards self-interstitials and different mobility. These loops, consisting of collections of crowdions oriented along the Burgers vector direction, are formed in different proportion depending on Cr concentration. The separation of a coherent, Cr-rich phase, denoted as  $\alpha'$  (at  $C_{Cr} > 10\%$ ) has also been claimed to be related to void formation resistance [6]. Radiation-accelerated formation of Cr-rich bcc precipitates is indeed known to occur within a certain range of temperature and Cr concentration, depending on dose. Primary  $\alpha'$  nuclei are finely dispersed particles of nanometric size typically having about 85–95% of Cr in them [7]. However, no qualitative relationship between either explanation and the actual swelling behaviour observed in Fe–Cr alloys has yet been found or proposed.

Recently, an analytical model for the assessment of self-interstitial cluster mobility in Fe–Cr alloys has been developed, based on the result of molecular static calculations with an early Fe–Cr potential [8]. The model is built on the idea that an attractive interaction exists between Cr atoms and crowdions in interstitial clusters, as shown also by *ab initio* calculations. Within such a model, the strong decrease of the diffusivity of small, one-dimensionally gliding SIA clusters was shown to be correlated with the reduction of swelling in the 1–10% Cr range. However, this model did not account for either the presence of the  $\alpha'$  or the cluster size effects, so it could only be used in a limited region of  $C_{Cr}$ .

Lately, the application of *ab initio* techniques allowed an advanced semi-empirical potential (based on the two-band model) to be parameterized [9]. It has been proven capable of reproducing the specific thermodynamic behaviour of the Fe–Cr system in the full range of Cr concentrations [9], including  $\alpha'$  precipitation, and of providing at the same time very good results for point defect properties as compared to *ab initio* predictions. To describe Fe–Fe interactions, a recently developed potential which was especially improved for the description of point defect properties was chosen [10,11]. We used this Fe–Cr potential to continue our molecular static (MS) and molecular dynamics (MD) investigation of the effect of Cr on the migration of self-interstitial clusters and small dislocation loops. In particular, the focus has been put on the effects of cluster size and Cr-rich precipitates on cluster

mobility. It is shown that by allowing for these effects an explanation for the experimentally observed swelling behaviour versus Cr content at different doses can be provided.

## 2. Methodology

### 2.1. *Ab initio* calculations

*Ab initio* calculations have been performed specifically to study the strength and range of the Cr-crowdion interaction. Density functional theory (DFT) is an eminent tool for studying these kinds of properties, totally inaccessible to experiments, and is the only *ab initio* method which is fast enough and includes all the relevant physics (especially spin polarisation). DFT was therefore applied, using the projector augmented wave (PAW) approach [12] implemented in the Vienna *Ab initio* Simulation Package (VASP) [13]. The calculations were spin polarised and the exchange-correlation functional used was the generalized gradient approximation (GGA) of Perdew and Wang [14]. 27 *k*-points were sampled according to the algorithm by Monkhorst and Pack [15]. The energy cutoff was 300 eV. Periodic boundary conditions were applied to a non-cubic supercell containing 121 atoms. The choice of the supercell and the applied constraints were dictated by the problem to be studied. Thus, the supercell had the [110], [112] and [111] vectors as coordinate basis vectors. The [111] pseudoplane (spanned by the [110] and [112] vectors) was 0.80 times 0.69 nm large and consisted of 12 atoms in three layers. The whole box consisted of 10 such layers and was 2.45 nm long, consistently with the DFT equilibrium lattice parameter equal to 2.823 Å. This geometry allowed the largest Cr-crowdion distance possible along the [111] direction to be considered within the computing time limitations imposed by DFT calculations. The  $\langle 111 \rangle$  SIA was constrained to move only in the  $\langle 111 \rangle$  direction, since it otherwise would relax to a  $\langle 110 \rangle$  SIA. Moreover, in order to obtain the binding energy of a nearest neighbour Cr to the SIA, avoiding the latter to move towards the Cr atom, the defect had to be constrained in all directions and only local relaxations of the remaining atoms were allowed (at constant volume). Therefore, the exact values obtained are not quantitatively fully reliable, but the trend is. However, similar calculations have been performed in a standard cubic box, without constraints and after thoroughly checking the

convergence for the chosen amount of  $k$ -points, finding very similar and fully consistent results. For consistency, exactly the same constraints have been applied in MS simulations to compare the results obtained using the interatomic potential with the *ab initio* ones; the only difference was that in the MS calculations the equilibrium lattice parameter given by the potential, 2.8553 Å, was used.

## 2.2. MS and MD calculations

Using a MS technique a set of binding energies of self-interstitial clusters of different sizes in Fe–Cr alloys was calculated to estimate the change in the cluster free energy using the definition proposed in Ref. [8]:

$$\Delta F_n = k_B T [(-E_b(x)/k_B T)], \quad (1)$$

where  $E_b(x)$  is the binding energy of the SIA cluster (of size  $n$ ) in a particular configuration  $x$  and brackets denote averaging over different configurations. More specifically, the binding energies entering Eq. (1) were defined as the differences between the maximum energy state encountered in the box, while changing the random local Cr atom distribution, and the energy in each configuration. The objective of this calculation was to obtain the data necessary to predict the diffusivity of self-interstitial clusters as a function of size in Fe–Cr solid solutions of different concentrations, using the model developed in [8].

Simulation boxes of rectangular shape with axes along  $[111]$ ,  $[11\bar{2}]$  and  $[1\bar{1}0]$  directions and 3D periodic boundary conditions were used for the static calculations. The box side length was 25–40 $a_0$  along  $[11\bar{2}]$  and 14–50 $a_0$  along  $[1\bar{1}0]$  directions, where  $a_0$  is the lattice parameter of bcc Fe, equal to 0.28553 nm at  $T = 0$  K for the potential set used. Along the orthogonal  $[111]$  direction the box side length varied from 50 $b$  to 100 $b$ , depending on the size of the SIA cluster. The corresponding number of bcc lattice sites ranged thus from 30000 to 800000. Calculations were carried out for clusters of hexagonal shape consisting of 7–91 SIAs, for Cr concentrations up to 25 at.% Cr atoms, randomly distributed in the box.

In the case of the interaction of Cr-rich precipitates with SIA clusters and small dislocation loops, static calculations have been performed to estimate the interaction energy depending on the distance between precipitate and SIA cluster and their sizes. Dynamic simulations were performed to assess the

mechanism of interaction, namely, to clarify if the SIA cluster can pass through the precipitate or remains bound inside or at the edge of it. In both cases, the simulation box was chosen as described before (containing up to 800000 lattice sites). The sizes of the Cr-rich precipitates were chosen to range from 0.5 nm to 5.8 nm, following experimental indications [7], while the sizes of the SIA cluster varied from 7 to 331 interstitials. Two cases of geometry of interaction were considered, (1) when the centre of the cluster is on the same  $\langle 111 \rangle$  direction as the centre of the precipitate (concentric interaction) and (2) when the  $\langle 111 \rangle$  direction from the centre of the cluster is tangent to the interface between precipitate and matrix (eccentric interaction). The precipitates consisted of three Cr concentrations, namely, 85%, 90% and 95%, following available experimental measurements [7]. The simulation temperature was 600 K. The integration of the equations of motion was performed in the NVE ensemble at zero total pressure conditions with a constant time step of 0.5 fs and for a simulation time  $t_S$  of 5–30 ns. During the simulations, the coordinates of the interstitials were recorded every 10 fs. Using this information, the position of the cluster was tracked and the interaction between Cr-rich precipitate and cluster was followed using visualization tools.

## 3. Results

The above-mentioned model [8] predicts a decrease of the SIA cluster mobility in Fe–Cr alloys as compared to pure Fe based on the postulated existence of a relatively strong and long-range interaction between the  $\langle 111 \rangle$  crowdions in the clusters and Cr atoms located on the same  $\langle 111 \rangle$  direction. Calculations made using *ab initio* methods and the most recent Fe–Cr potential [10,11] confirmed the presence of this effect. Fig. 1 represents the binding energy of the crowdion with a Cr atom as a function of the distance between them, calculated using both *ab initio* and interatomic potential based static techniques at a temperature of 0 K. The results obtained with the interatomic potential are given for four cases: isolated crowdion and crowdion in a cluster containing 7, 37 and 91 self-interstitials. The binding energy given in Fig. 1 corresponds to the case when the Cr atom interacts with a crowdion located at the edge of the cluster, since the strongest interaction is expected in this region. In the centre of a cluster the weakest interaction is foreseen [16]. The interaction energy is lower for the crowdion in the

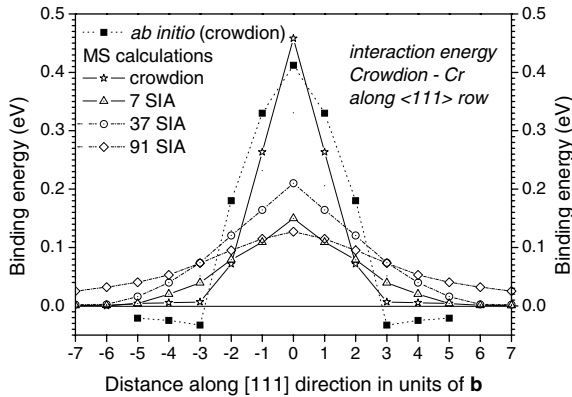


Fig. 1. The binding energy of a crowdion with a Cr atom as a function of the distance between Cr atom and crowdion calculated using *ab initio* and molecular static techniques. Crowdions were considered both individually and in clusters of different sizes, located at the edge of it. Positive values denote attraction.

cluster than for the isolated one, but the interaction distance is longer in the cluster. This is the consequence of the slightly different structure of the crowdions in the cluster, due to the perturbation caused by neighbouring crowdions. The maximum binding energy between the Cr and SIA clusters occurs when the Cr atom is inside the cluster, or in the middle of a crowdion.

Because of such interaction, the 1D migration of a cluster in a Fe–Cr alloy can be represented as the motion in a field of energy valleys and hills, representing different energy states of the cluster, corresponding to different numbers of Cr atoms interacting with it. The height and distance between those valleys and hills will mainly depend on cluster size and Cr concentration. This hypothesis was also the basis for the mentioned analytical model [8]. The time a cluster spends in a particular configuration inside the Fe–Cr matrix is assumed to be proportional to  $\exp(\beta\Delta F_n)$ , where  $\beta = (k_B T)^{-1}$ ,  $k_B$  is the Boltzmann constant,  $T$  is the absolute temperature and  $\Delta F_n$  is the change in the system free energy with regard to the lowest energy state. The diffusivity,  $D_n^{\text{FeCr}}$ , of a cluster of  $n$  SIAs in the alloy can thus be expressed as a function of that in pure Fe,  $D_n^{\text{Fe}}$ , as:

$$D_n^{\text{FeCr}} = D_n^{\text{Fe}} \exp(\Delta F_n / k_B T), \quad (2)$$

Changes in the cluster free energy versus Cr concentration are shown in Fig. 2, for clusters of 7, 19, 37, 61 and 91 self-interstitials, calculated putting

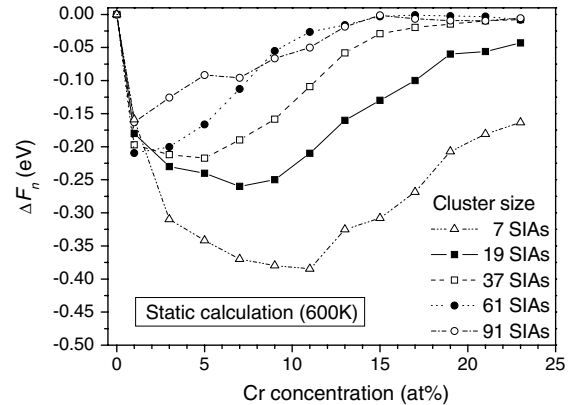


Fig. 2. Change in the free energy of SIA clusters of different sizes in an Fe–Cr alloy as a function of Cr concentration calculated using Eq. (1) at 600 K.

MS data in Eq. (1). Applying Eq. (2), one can immediately convert these results into the diffusion coefficient of the cluster of corresponding size. On the whole, one can see that the  $\Delta F_n$  are non-monotonic functions of the Cr concentration and that the location of their minima depends on the cluster size. The minima become shallower and their positions shift towards lower concentrations with increase of the cluster size. This translates into a non-monotonic decrease of the diffusivity of SIA clusters in Fe–Cr versus Cr concentration as compared to pure Fe, with a minimum at lower concentration: the larger the cluster size, the lower the  $C_{\text{Cr}}$  where the minimum is located. In addition, the influence of Cr on the cluster diffusivity gradually disappears for larger Cr contents. These effects are the consequence of two facts. On the one hand, for a given cluster size, adding Cr will initially increase the number of interacting Cr-crowdion, thereby increasing the binding energies, until a free energy minimum is reached when each crowdion in the cluster sees one Cr atom (see Eq. (1)). After this point, each crowdion will see more than one Cr atom and the effective binding energy will decrease, due to saturation of the interactions. On the other hand, the Cr distribution seen by clusters of increasing size becomes more and more uniform. Thus, the effective binding energy decreases and the free energy minimum shifts to lower Cr concentration.

It can be seen from Fig. 2 that the saturation of the Cr-crowdion interaction occurs for  $C_{\text{Cr}} > 12\%$ . In this range of concentrations another important radiation-induced phenomenon starts to occur, namely the separation of  $\alpha'$  phase.

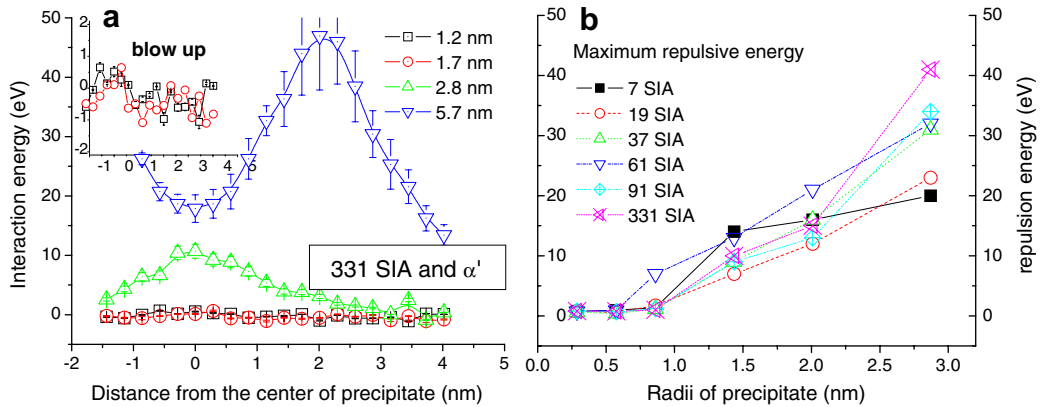


Fig. 3. Interaction energy between an SIA cluster and precipitates (with 90% Cr) as a function of the distance between them (a) and maximum repulsion energy between SIA clusters of different size and precipitates as a function of the precipitates' size (b). Positive sign means repulsion.

The interaction between SIA clusters and  $\alpha'$  precipitates and its effect on the fast 1D migration of self-interstitial clusters should therefore be allowed for, in order to have a complete picture, particularly considering the experimentally observed high density of these precipitates.

Fig. 3(a) displays the interaction energy between an SIA cluster of 331 interstitials and precipitates of different size (containing 90% Cr) in Fe–15% Cr as a function of distance, for the case when the centres of the SIA cluster and of the precipitate coincide. One can see that strong repulsion occurs when the cluster approaches the precipitate. By increasing the precipitate size, the barrier increases as well. The maximum repulsive energy was found when the SIA cluster was located at the interface between the precipitate and the matrix. In that case one side of the cluster platelet is still in the matrix, while the other side is in the Fe–90% Cr precipitate. We have also calculated the formation energy of SIA clusters in Cr-rich and Fe-rich alloys. The results revealed that the formation energy is significantly higher in Cr-rich regions. We believe that this might be the origin of the observed repulsion between clusters and precipitates.

The average values of the maximum repulsive energy between clusters and precipitates of different sizes in Fe–10%, 12% and 15% Cr are given in Fig. 3(b). The averaging was made over the two considered geometries of interaction. We have found that neither the nominal Cr concentration of the alloy, nor the cluster size change the sign of the interaction energy, which was found to be always strongly repulsive and growing with increas-

ing precipitate size. These energy barriers are generally much higher than the migration energy of small SIA clusters (up to 100 SIAs with  $E_m \sim 0.05$  eV [17]). So these clusters will move away from these obstacles. Exceptions could be very large clusters (331 SIA), corresponding to small observable dislocation loops, whose migration energy in pure Fe has been experimentally estimated to be about 1.3 eV (for a 6 nm  $\langle 111 \rangle$  loop [18]) and is therefore comparable with, or higher than, the barrier to overcome small precipitates (see Fig. 3(a)). These clusters will have a similar probability to move away from or to overcome the small precipitates.

The dynamic studies confirmed the expectations from static calculations: In the limit of the studied conditions, we did not see any cluster moving through a precipitate. The presence of the repulsive interaction was clearly revealed by the fact that clusters created very close to the precipitate rapidly moved away from it, while in the region of negligible interaction the normal 1D migration mechanism, with equally probable forward and backward jumps, was observed. In no case did any cluster move back towards the precipitate.

#### 4. Discussion: correlation to swelling behaviour

Our results show that the mobility of SIA clusters and small dislocation loops decreases in Fe–Cr compared to Fe. We would like to emphasize that a strong suppression of small dislocation loop motion in Fe–Cr compared to Fe has also been proven experimentally [19]. At the same time, the rate of growth of dislocation loops in Fe–Cr has been

found to be slower than in pure Fe, but leading to a much higher density, an effect that can also be ascribed to lower mobility [20]. These experiments were made under electron irradiation, in conditions where dislocation loops of interstitial nature are known to be formed.

A strong reduction of SIA cluster and small dislocation loop mobility leads to a pronounced decrease of cluster annihilation at dislocations, grain boundaries and other sinks. At the same time, it provides additional recombination sites for freely migrating vacancies and small vacancy clusters. Clearly, the combination of both effects will drastically reduce void swelling. In particular, three effects should be emphasized. In the random solution limit, the decrease of cluster diffusivity is non-monotonic: (i) Small SIA clusters, such as those directly formed in cascades initiated by fast neutrons, exhibit diffusivity minima in the 9–12% Cr range; (ii) with the increase of the cluster size the minima shift towards lower Cr concentrations, (iii) the interaction between fine Cr-rich precipitates and small dislocation loops is strongly repulsive: in conditions where fine, dispersed  $\alpha'$ -nuclei are formed, a strong suppression of small dislocation loop mobility should therefore also be expected because, being 1D migrating defects, such clusters will get 'locked' between  $\alpha'$  particles.

By combining these three observations, the general picture of void swelling behaviour versus Cr content can be built. Effect (i) explains the swelling minimum experimentally observed at relatively low doses (1–10 dpa) around 10% Cr (see Fig. 4), where

$\alpha'$  formation is not expected. With increasing dose, the average size of self-interstitial clusters will also increase (note that most of them are invisible in transmission electron microscopy). As a consequence of effect (ii), the swelling minimum will correspondingly shift towards lower concentration, in the range where  $\alpha'$ -precipitation cannot occur. However, in higher Cr-content alloys radiation-induced precipitation will appear with increasing dose. This will determine the appearance of another swelling minimum in correspondence with the concentration where the largest amount of dispersed, fine  $\alpha'$  precipitates is created. Thus, the variation of the swelling curves versus Cr content with dose, with one minimum around 10% Cr at lower dose and two separated minima at higher doses (see Fig. 4) can be explained. The possible further increase of swelling for  $C_{Cr} > 16\%$  could be the consequence of the coalescence of fine, dispersed  $\alpha'$ -nuclei into bigger precipitates, leading to lower precipitate density. Of course, temperature will also have a role in shifting the concentration where the different phase transformations are to be expected, as well as in affecting the time required for them to take place. Above a certain Cr concentration Fe–Cr alloys are known to undergo spinodal decomposition. This situation, however, has not been considered in the present work and may be the focus of future investigations.

## 5. Conclusions

The strong reduction of swelling in Fe–Cr alloys and its dependence on Cr content has been explained in terms of an enhanced recombination of vacancies on SIA clusters and small dislocation loops of reduced mobility. The diffusivity of these objects is strongly reduced by the presence of Cr in the solid solution, due to the attractive interaction between crowdions and Cr atoms. The observed strong repulsion with  $\alpha'$ -precipitates, on the other hand, which provides an array of obstacles for the SIA clusters to freely move, prevents cluster annihilation at extended sinks in the concentration region where phase separation occurs.

We believe that our reasoning is adequate to explain the main observed trends in the void swelling curve versus Cr content in Fe–Cr alloys. Investigation of the effect of Cr on the formation of  $\langle 100 \rangle$  loops, their migration properties and their possible influence on swelling behaviour is the next issue to be investigated.

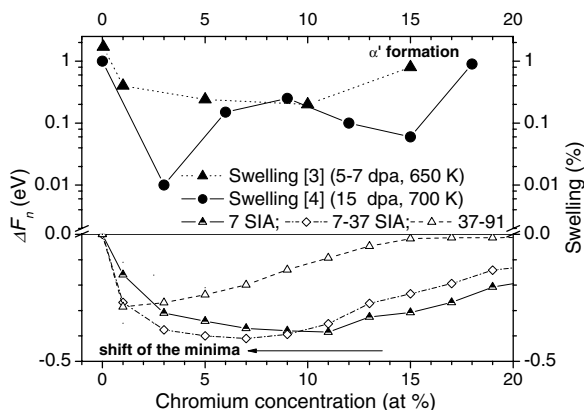


Fig. 4. Change in the free energy of clusters in an Fe–Cr alloy compared to swelling from Refs. [3,4] as a function of Cr concentration.

## Acknowledgements

This work, partially supported by the European Commission under the contract of Association between Euratom and the Belgian State, was carried out within the framework of the European Fusion Development Agreement (EFDA), task TTMS-007, P. Olsson acknowledges the Swedish National Allocations Committee for the use of supercomputer facilities, A.V. Barashev acknowledges a research grant from the UK Engineering and Physical Sciences Research Council.

## References

- [1] G.W. Greenwood, A.J.E. Foreman, D.E. Rimmer, *J. Nucl. Mater.* 4 (1959) 305;  
C. Cawthorne, E.J. Fulton, *Nature* 216 (1967) 575.
- [2] B.N. Singh, *Radiat. Eff. Def. Solids* 148 (1999) 383;  
H. Trinkaus, B.N. Singh, A.J.E. Foreman, *J. Nucl. Mater.* 199 (1992) 1.
- [3] E.A. Little, D.A. Stow, *J. Nucl. Mater.* 87 (1979) 25.
- [4] D.S. Gelles, *J. Nucl. Mater.* 108&109 (1982) 515.
- [5] F.A. Garner, M.B. Toloczko, B.H. Sencer, *J. Nucl. Mater.* 276 (2000) 123.
- [6] R. Bullough, M.H. Wood, E.A. Little, in: D. Kramer, H.R. Brager, J.S. Perrin (Eds.), *Effects of Radiation on Materials: Tenth Conference*, ASTM STP 725, ASTM, Philadelphia, 1989, p. 593;
- D.S. Gelles, in: N.H. Packan, R.E. Stoller, A.S. Kumar (Eds.), *Effects of Radiation on Materials: 14th International Symposium*, ASTM STP 1046, vol. I, ASTM, Philadelphia, 1989, p. 73.
- [7] M.H. Mathon, Y. de Carlan, G. Geoffroy, X. Averty, C.H. de Novion, *J. Nucl. Mater.* 312 (2003) 236;  
P. Dubuisson, D. Gilbon, J.L. Séran, *J. Nucl. Mater.* 205 (1993) 178.
- [8] D. Terentyev, L. Malerba, A.V. Barashev, *Philos. Mag. Lett.* 85 (2005) 587.
- [9] P. Olsson, J. Wallenius, C. Domain, K. Nordlund, L. Malerba, *Phys. Rev. B* 72 (2005) 214119.
- [10] G.J. Ackland, M.I. Mendelev, D.J. Srolovitz, S. Han, A.V. Barashev, *J. Phys.: Condens. Matter* 16 (2004) S2629.
- [11] F. Williame, C.C. Fu, M.C. Marinica, J. Dalla Torre, *Nucl. Instrum. and Meth. B* 228 (2005) 92.
- [12] G. Kresse, D. Joubert, *Phys. Rev. B* 59 (1999) 1758.
- [13] G. Kresse, J. Hafner, *Phys. Rev. B* 47 (1993) 558.
- [14] J.P. Perdew, Y. Wang, *Phys. Rev. B* 45 (1991) 13244.
- [15] H.J. Monkhorst, J.D. Pack, *Phys. Rev. B* 13 (1976) 5188.
- [16] M.A. Puigvi, Yu.N. Osetsky, A. Serra, *Philos. Mag. A* 83 (2003) 857.
- [17] Yu. N. Osetsky, D.J. Bacon, A. Serra, B.N. Singh, S.I. Golubov, *Philos. Mag. A* 83 (2003) 61.
- [18] K. Arakawa, personal communication, 2006.
- [19] K. Arakawa, M. Hatanaka, H. Mori, K. Ono, *J. Nucl. Mater.* 329–333 (2004) 1194.
- [20] N. Yoshida, A. Yamaguchi, T. Muroga, Y. Miyamoto, K. Kitajama, *J. Nucl. Mater.* 155–157 (1988) 1232.